TITLE: Toward a Molecular Understanding of the Mechanism of Cryopreservation by Polyampholytes: Cell Membrane Interactions and Hydrophobicity

AUTHOR NAMES: Robin Rajan[1], Fumiaki Hayashi[2], Toshio Nagashima[3], Kazuaki Matsumura[1]*

AUTHOR ADDRESSES:

[1]School of Materials Science, Japan Advanced Institute of Science and Technology, 1-1 Asahidai, Nomi, Ishikawa 923-1292, Japan

[2]NMR Facility, Division of Structural and Synthetic Biology, RIKEN Center for Life Science Technologies, 1-7-22 Suehiro-cho, Tsurumi-ku, Yokohama City, Kanagawa, 230-0045, Japan

[3]NMR Facility Support Unit, NMR Facility, Division of Structural and Synthetic Biology, RIKEN Center for Life Science Technologies, 1-7-22 Suehiro-cho, Tsurumi-ku, Yokohama City, Kanagawa, 230-0045, Japan

*To whom correspondence should be addressed:

Kazuaki Matsumura

E-mail address: mkazuaki@jaist.ac.jp

Tel.: +81-761-51-1680

Fax: +81-761-51-1149

ABSTRACT: Cryopreservation enables long-term preservation of cells at ultra-low temperatures. Current cryoprotective agents (CPAs) have several limitations, making it imperative to develop CPAs with advanced properties. Previously, we developed a novel synthetic polyampholyte based CPA, copolymer of 2-(dimethylamino)ethyl methacrylate (DMAEMA) and methacrylic acid(MAA), (poly-(MAA-DMAEMA)) which showed excellent efficiency and biocompatibility. Introduction of hydrophobicity increased its efficiency significantly. Herein, we investigated the activity of other polyampholytes. We prepared two zwitterionic polymers, poly-sulfobetaine (SPB) and poly-carboxymethyl betaine (CMB) and compared its efficiency with poly-(MAA-DMAEMA). Poly-SPB showed only intermediate property and poly-CMB showed no cryoprotective property. These data suggested that the polymer structure strongly influences cryoprotection, providing an impetus to elucidate the molecular mechanism of cryopreservation. We investigated the mechanism by studying the interaction of polymers with cell membrane, which allowed us to identify the interactions responsible for imparting different properties. Results unambiguously demonstrated that polyampholytes cryopreserve cells by strongly interacting with cell membrane, with hydrophobicity increasing the affinity for membrane interaction, which enable it to protect the membrane from various freezing induced damages. Additionally cryoprotective polymers, especially their hydrophobic derivatives, inhibit the recrystallization of ice, thus averting cell death. Hence, our results provide an important insight into the complex mechanism of cryopreservation, which might facilitate the rational design of polymeric CPAs with improved efficiency.

KEYWORDS: cryoprotective agent, hydrophobicity, membrane, polyampholyte, polymer, zwitterionic

INTRODUCTION

Our current understanding of cryopreservation stems from the studies performed over the last two centuries. The first successful cryopreservation was reported by Polge et al. in 1949 when the authors serendipitously discovered the cryoprotective property of glycerol on fowl sperm.[1] A few years later, Lovelock et al. reported dimethyl sulfoxide (DMSO) as an efficient cryoprotectant for red blood cells.[2] Since then, numerous research groups undertook investigations to explain the physical phenomenon[3, 4] and kinetics behind cryopreservation.[5-9] However, both glycerol and DMSO have certain issues. Glycerol is a relatively weaker CPA and DMSO shows high cytotoxicity[10] and affects differentiation of various kinds of cells,[11] hence it needs to be eliminated rapidly after thawing. Due to the absence of efficient alternatives to DMSO, it is still used frequently as the preferred cryoprotective agent (CPA) in many biological applications. Thus, development of newer and more efficient CPA is of paramount importance.

Recently, Matsumura et al. developed a non-penetrating polymer-based cryoprotectant, carboxylated poly-l-lysine (COOH-PLL), which has both positive and negative charges on the polymer chain (a polyampholyte).[12] It was found to be an excellent CPA with various cell types, even in the absence of any antifreeze proteins like fetal bovine serum (FBS). The cells showed a good survival rate even after cryopreservation for 24 months.[13] Dextran-based polyampholytes also exhibited excellent cryoprotective property,[14] although the molecular mechanism of cryopreservation was not elucidated.

Polyampholytes are a special class of polymers bearing both positive and negative charges. They may be either neutral in charge or have a net charge. A tremendous increase in research in the field of polyampholytes has arisen recently because it their properties can be fine-tuned

by incorporating particular monomer subunits. This can be achieved by developing random copolymers or block-copolymer systems with different ratios of monomers of various molecular mass distributions. Thus, polyampholytes have found applications in a plethora of fields including catalysis, water desalination, and a wide range of other applications. Polyampholytes have also been used in a variety of biomedical applications.[15, 16] A sub-class of polyampholytes that has recently received attention are zwitterionic polymers, which have the same number of anionic and cationic groups within a single repeating unit. In polyampholytes, cationic and anionic sites may be scattered randomly along the polymer chain and the charges of 1 ion may exceed that of the other ion, leading to the formation of charged polymers. Another difference is that with polyampholytes, the charge of the polymer backbone can be easily adjusted by changing the ratio of the 2 component monomers and the net charge of the polymer may be either positive, negative, or zero; however, with zwitterionic polymers, the net charge is usually zero under normal pH conditions. This property of zwitterionic polymers is due to the presence of an equal number of positive and negative charges within the polymer; therefore, they display a hybrid-like property profile, which is due to the presence of numerous polymer-bound ion pairs attached to the polymer chain. Zwitterionic polymers are governed by strong Coulomb interactions resulting in high hydrophilicity.[17]

Previously, we developed a synthetic polyampholyte cryoprotectant via living free-radical polymerization, which showed good cell viability and biocompatibility. Incorporating a low percentage of hydrophobic moieties led to a significant increase in cell viability.[18] However, the mechanism of polyampholyte-mediated cryopreservation was not determined, imposing a limit to the rational development of polyampholytes with improved cryoprotective properties. Establishing the underlying molecular mechanism of cryoprotectants could assist in the employment of these polyampholytes for various regenerative medicines like stem cell

cryopreservation, tissue engineering, and the development of cellular scaffolds. Moreover, such mechanistic insights could help in the more efficient design of CPAs in the future, wherein newer materials could be put into use with the current knowledge. In addition, these polymers can be modified for the cryopreservation of cell-containing constructs. Gibson et al. suggested that ice recrystallization inhibition (IRI) by polyampholytes enable them to successfully cryopreserve red blood cells.[19]

In this study, we investigated the role of polymer structures in cryopreservation. To this end, we formulated structurally analogous polyampholytes with modest structural differences by RAFT polymerization and compared their activities with a previously synthesized polyampholyte, copolymer of 2-(dimethylamino)ethyl methacrylate (DMAEMA) and methacrylic acid(MAA) (poly-(MAA-DMAEMA)).[18] Hydrophobicity was also introduced into the polymers using hydrophobic moieties, such as n-butyl methacrylate (BuMA) and n-octyl methacrylate (OcMA). We demonstrated that the cryopreservation efficiency depends not only on the IRI activity of the polyampholytes, but also on cell membrane protection. Based on these insights, we investigated both membrane interactions and IRI. Liposomes were used to probe the interaction of polyampholytes with the cell membrane during freezing. The effects of various polymers on freezing was also evaluated by studying the ice recrystallization during thawing (by cryomicroscopy), which is lethal to cell membrane and causes subsequent cell death. The interaction of polyampholytes with the cell membrane and their relative subcellular localization was investigated with differential scanning calorimetry (DSC) and electron spin resonance (ESR) spectroscopy. Direct membrane protection/lysis during freezing was analyzed by performing leakage experiments. Investigating structure-function relationships of polymers with respect to their cryopreservation efficacy can shed further insights into the molecular mechanism of cryopreservation.

MATERIALS AND METHODS

Materials

The compounds 2-(dimethylamino)ethyl methacrylate (DMAEMA), methacrylic acid (MAA), and n-butyl methacrylate (BuMA) were purchased from Wako Pure Chemical Industries, Ltd. (Osaka, Japan). N-octyl methacrylate (OcMA) was purchased from NOF Corporation (Tokyo, Japan). All of these monomers were distilled under reduced pressure prior to use to remove polymerization inhibitors. Sulfobetaine (SPB) and carboxymethyl betaine (CMB) were donated by Osaka Organic Chemical Industry, Ltd. (Osaka, Japan). The compounds 2-(dodecylthiocarbonothioylthio)-2-methylpropionic acid, 5- and 16-doxyl stearic acid (DSA), and carboxyfluorescein (CF) were purchased from Sigma–Aldrich (St. Louis, MO, USA) and used as provided without further purification. The compound 4–4′-azobis-(4-cyanovaleric acid) (V-501, initiator) was purchased from TCI (Tokyo, Japan). Azobisisobutyronitrile (AIBN) was purchased from Wako. AIBN was recrystallized with methanol before using. Egg phosphatidylcholine (EPC) was purchased from NOF Corporation. Ethanol, methanol, 2-propanol, and Triton® X-100 were purchased from Nacalai Tesque Inc. (Kyoto, Japan).

Synthesis of Polyampholytes

Synthesis of poly-(MAA-DMAEMA), a Copolymer of Methacrylic Acid (MAA) and 2-(Dimethylamino)Ethyl Methacrylate (DMAEMA)

Poly-(MAA-DMAEMA) was prepared as described in our previous study.[18] Briefly, DMAEMA, MAA, 2-(dodecylthiocarbonothioylthio)-2-methylpropionic acid (RAFT agent), and V-501 (initiator) were added to a reaction vial, after which 20 mL of a 1:1 (v/v) water–methanol mixture was added. The solution was purged with nitrogen gas for 1 h and stirred at 70 °C for 24 h. The reaction mixture was then precipitated using 2-propanol, the precipitate was collected by centrifugation, and the compound was dried in a vacuum (Scheme 1a).

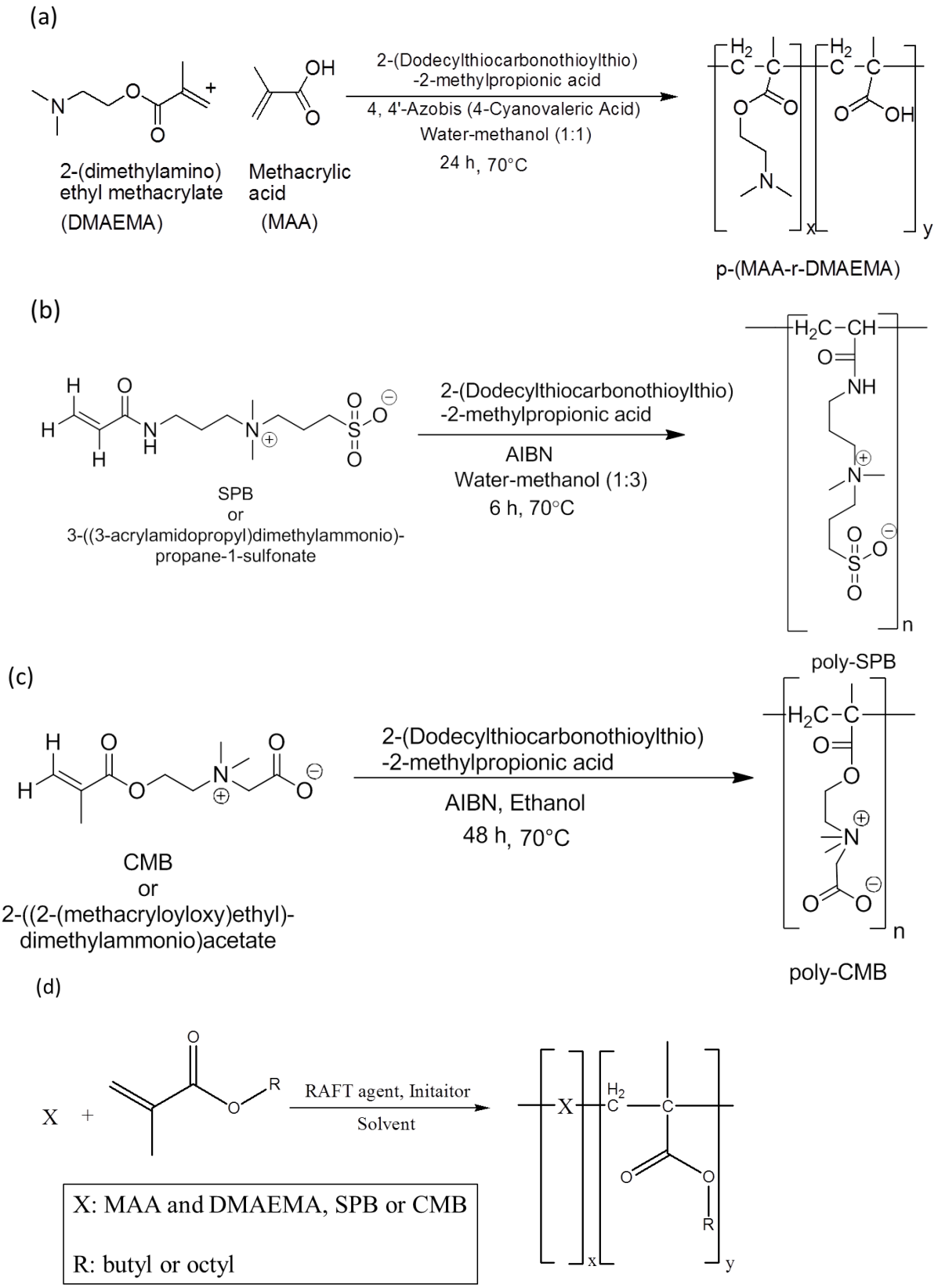

Scheme 1. Synthesis of (a) poly-(MAA and DMAEMA) (b) poly-SPB, (c) poly-CMB, and (d) hydrophobic derivatives of polyampholytes by RAFT polymerization

Synthesis of poly-SPB

The SPB monomer 2-(dodecylthiocarbonothioylthio)-2-methylpropionic acid and AIBN were dissolved in a 3:1 (v/v) methanol-water mixture. The solution was then purged with nitrogen gas for 1 h and stirred at 70 °C for 6 h. The reaction mixture was then dialyzed successively against methanol and water for 24 h each, with constant change of solvent. The polymer was then obtained after lyophilization (Scheme 1b).

Synthesis of poly-CMB

The CMB monomer 2-(dodecylthiocarbonothioylthio)-2-methylpropionic acid and AIBN were dissolved in ethanol. The resulting solution was purged with nitrogen gas for 1 h and stirred at 70 °C for 48 h. The reaction mixture was then precipitated using 2-propanol, precipitate was collected by centrifugation, and the compound was dried in a vacuum (Scheme 1c).

Introduction of Hydrophobicity

Hydrophobic derivatives of the above 3 polymers were synthesized by including either the hydrophobic BuMA or OcMA monomer to the reaction mixture and then proceeding with the polymerization. A hydrophobicity of 2–5 % was introduced by adding different amounts of hydrophobic monomers (Scheme 1d).

Molecular Weight Determination

The molecular weight and distribution (polydispersity index) of the polymers were determined by gel-permeation chromatography (GPC; BioSep-SEC-s2000 column, Phenomenex, Inc., Torrance, CA, U.S.A.) and was measured using a Shimadzu high-

performance liquid chromatography data system equipped with a refractive index detector. A phosphate buffer (pH 7.4, 0.1 M) was used as the mobile phase for poly-(MAA-DMAEMA), and NaBr solution (pH 7.4, 0.1 M) was used as the mobile phase for poly-CMB and poly-SPB (flow rate, 1 mL min^{-1}). Pullulan (Shodex Group, Tokyo, Japan) was used as the standard.

Cell Culture and Cryopreservation

L929 cells (American Type Culture Collection, Manassas, VA, USA) were cultured in Dulbecco's Modified Eagle's Medium (DMEM, Sigma Aldrich) supplemented with 10% FBS. Cells were cultured at 37°C in a CO_2 incubator in a humidified atmosphere. When the cells were confluent, they were washed with phosphate buffered saline (PBS) and then treated with trypsin solution (0.25 % [w/v] trypsin containing 0.02 % [w/v] ethylenediaminetetraacetic acid in PBS) to detach the cells. The cell pellet was then collected by centrifugation, mixed with fresh DMEM, and subsequently transferred to a new culture plate for subculture.

Polyampholyte solutions were prepared in DMEM without FBS at concentrations ranging from 2.5–15 % [w/v]. The pH of the solution was adjusted to 7.4, and the osmotic pressure was adjusted to 500 mmol/kg by the addition of sodium chloride using a vapor pressure osmometer (VAPRO Model 5660, WESCOR Biomedical Systems, Logan, UT, U.S.A.). These solutions were filter-sterilized using a 0.22-μm MILLEX GP Filter Unit (Millipore Corp., Billerica, MA, U.S.A.). One million L929 cells were suspended in 1 mL of each cryopreservation solution in a vial and stored at −80 °C without controlling the cooling rate. After 1 week, the vials were thawed in a water bath maintained at 37 °C with gentle shaking. Cell suspensions were then diluted tenfold and mixed well, and then the cell pellet was

collected by centrifugation. The cells were stained with trypan blue and counted on a hemocytometer. Cell viability was reported as the ratio of viable cells to the total number of cells, and the percent cell viability was calculated.

Liposome Preparation

EPC (12 mg) was dissolved in chloroform, in a glass test tube. The chloroform solvent was evaporated under a gentle stream of nitrogen gas to produce a thin lipid film. The film was subsequently dried overnight under a vacuum. The resulting lipid film was hydrated in aqueous solution, and single unilamellar vesicles were obtained using a mini-extruder set (Avanti Polar Lipids) and membranes with a 0.1 μm pore size. Liposomes are closed vesicles made up of phospholipid bilayers and enclose an aqueous solution; hence, they are commonly used as a cell membrane mimic.

DSC experiments

The thermal behavior of the lipids in the presence of polyampholytes was studied by DSC. Thermograms of EPC liposomes with polyampholytes were obtained at polymer/EPC mass ratios between 0 and 1.0. Fifty microliters of each sample was transferred to an alodined aluminum pan, and measurements were taken using a Seiko Instrument EXTAR SII-6200 DSC system in a temperature range of −30 °C to 80 °C, with a heating rate of 20 °C/min in a constant nitrogen flow. The gel-to-liquid phase transition temperature of the lipid was recorded as the temperature at the peak minimum.

ESR Spectroscopy

EPC (0.013 mmol) was dissolved in 1 mL chloroform, after which 1×10^{-4} mmol of 5-DSA or 16-DSA was added to prepare the corresponding spin-labeled liposomes. The chloroform

solvent was evaporated under a gentle stream of nitrogen gas to produce a thin lipid film. The film was subsequently dried under a vacuum overnight. The resulting lipid film was hydrated in aqueous solution, and single unilamellar vesicles were obtained using a mini-extruder set (Avanti Polar Lipids) and membranes with a 0.1 μm pore size. The liposomes were suspended in polyampholyte solutions of various concentrations and stored at −78 °C. After 24 h, solutions were thawed in a 37 °C water bath. The solutions were then transferred to an ESR quartz flat cell, equipped with a screw knob (ES-LC12; JEOL, Ltd., Tokyo, Japan). The flat cell was placed in the cavity of the spectrometer, and ESR spectra were recorded on a JEOL JES-FA100 ESR Spectrometer, using the following parameters: sweeping field, 333 ± 10 mT; microwave power, 10 mW; modulation width, 0.02 mT; sweep time, 2 min; total sweep, 10; time constant, 0.03 s; and amplitude, 1000.

We employed 2 kinds of nitroxide probes (5-DSA and 16-DSA), which are free fatty acids. The nitroxide group of 5-DSA acid becomes located near the polar head group region of the cell membrane,[20] so a change in probe mobility can assist in the detection of polyampholyte in this cellular region. The molecular motion in the 5-position of fatty acid chain is anisotropic and produces spectra where both outer and inner hyperfine extrema are defined,[21, 22] and order the parameter S may be calculated according to the following equation (Fig. 1a).

$$\mathbf{S} = \frac{A_{II} - A_I}{a} \times \mathbf{0.5407}\ \mathbf{,\ a = (A_{II} + 2A_I)/3}$$

where A_{II} and A_I are the apparent parallel and perpendicular hyperfine-splitting parameters, respectively. S represents the anisotropy of motion, which represents the ordering along the long molecular axis.[23]

In contrast, the radical group of 16-DSA becomes localized near the lipid core region of the phospholipid membranes. The molecular motion is isotropic and the spectra are highly

disordered, and as such, the correlation time (τ_c) is calculated according to the following equation (Fig. 1b).

$$\tau_c = (6.6 \times 10^{-10} W_0)\left[sqrt\left(\frac{h_0}{h_{-1}}\right) - 1\right]$$

where h_0/h_{-1} is the ratio of the peak heights of the central and high field lines, respectively, and W_0 is the peak-to-peak width of the central line. τ_c represents the motional rate parameter.[23]

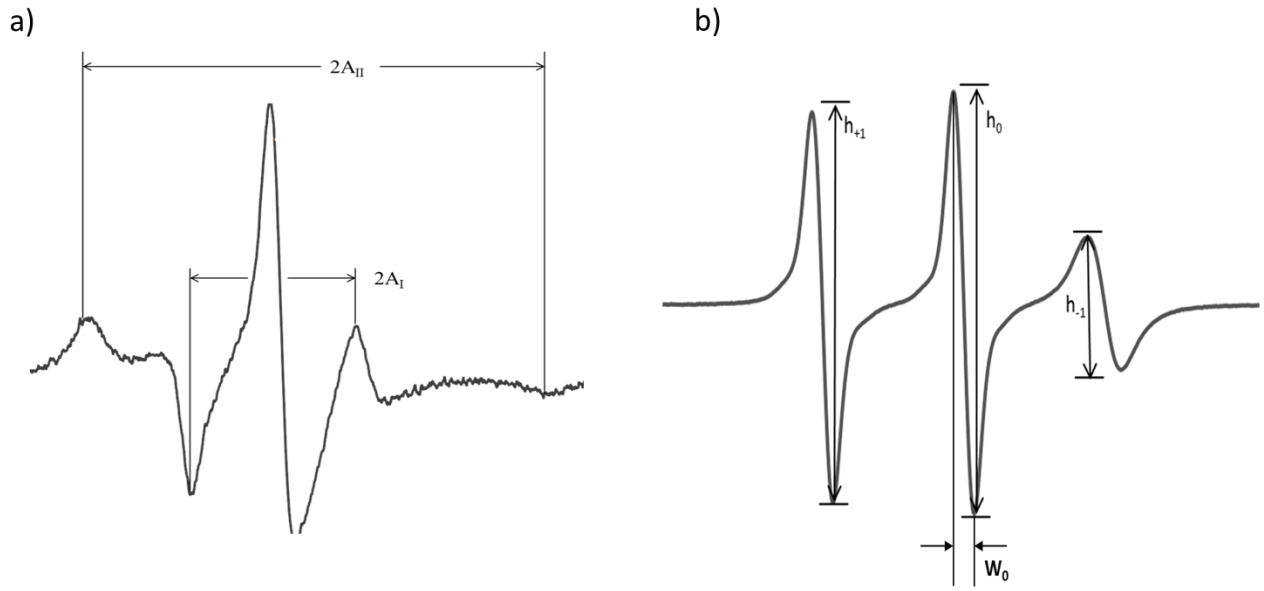

Figure 1. ESR spectra of (a) 5-DSA and (b) 16-DSA in EPC liposomes in PBS (pH 7.4)

IRI-Cooling Splat Assay

The potential of the polymers to inhibit ice recrystallization during freezing was examined using a modified splat assay. Briefly, 20 μL of a polymer sample dissolved in PBS was dropped from 1.5 m above a glass coverslip placed on a thin aluminum sheet on dry ice. Following droplet splatting onto the chilled coverslip, a thin wafer with a diameter of 10–12 mm formed immediately, which was composed of very fine-grained ice. The glass coverslip was then transferred to a Linkam Scientific cryostage and maintained at −6 °C. It was then

allowed to stabilize for 30 min under a nitrogen atmosphere. Photographs were captured using a Nikon DS Fi2 microscope fitted with crossed polarizers. The images were then processed using ImageJ software (National Institutes of Health, Bethesda, MD, U.S.A.). The degree of recrystallization was quantitatively analyzed by measuring the mean largest grain size (MLGS) from 5 individual wafers and was calculated relative to the size obtained using a PBS control.[24]

Leakage Experiment

Thin films of liposomes were prepared by the procedure described above. The resulting lipid film was hydrated in 600 μL of 0.1 M CF/PBS solution, and uniform liposomes were obtained using a mini-extruder set (Avanti Polar Lipids) and membranes with a 0.1 μm pore size. The excess of CF dye was removed by passing the liposome though a Sephadex G-25 column (NAP-5, GE Healthcare). The resultant liposomes were then suspended in polymer solutions of different concentrations and were stored at −80°C. The mixture was then thawed after 24 h in a 37 °C water bath. CF fluorescence was measured with a JASCO FP-8600 spectrofluorometer, using an excitation wavelength of 450 nm and a detection wavelength of 520 nm. Fluorescence quenching occurred when the membrane was intact (protected) after the freeze-thaw process, and an increase in fluorescence intensity represented membrane damage due to the release of CF into the surrounding buffer. Complete membrane lysis was determined (100 % leakage) after mixing with Triton X-100, and the percentage leakage for the other systems were calculated relative to these values.[18]

Statistical Analysis

All data are expressed as the mean ± standard deviation (SD). All experiments were conducted in triplicate. To compare data among more than 3 groups, 1-way analysis of

variance with the Tukey–Kramer test was used. Differences were considered statistically significant at a P value of < 0.05.

RESULTS AND DISCUSSION

Characterization

Polyampholytes were prepared under various conditions and characterized by ^{1}H-NMR, ^{13}C-NMR, and GPC. Reaction completion was monitored by ^{1}H-NMR by observing the loss of vinyl protons from the monomer (Fig. S1). Conversion of the monomer to the corresponding polymer and the ratio of the initial concentration to that measured at any given time during the reaction, $\ln([M]_o/[M])$, were also evaluated using ^{1}H-NMR. Poly-SPB formed the fastest, with the reaction being >80 % complete within the first 2 h, followed by poly-CMB, where the reaction was ~75 % complete after 2 h (Fig. 2). In contrast, poly-(MAA-DMAEMA) formed relatively slowly, with only 40 % conversion in the first 2 h. The plot of $\ln([M]_o/[M])$ vs. the reaction time showed a linear relationship, indicating the presence of constant number of active species during the polymerization.[25] The final polymers obtained were characterized by 2D-NMR (Fig. S2). A summary of the characteristics of the polymers is provided in Table 1. The compositions of each monomer in the polymers were well controlled and were in accordance with the initial feed ratio. Furthermore, the GPC curves indicated that all the polymers had a unimodal distribution with polydispersity index (M_w/M_n) in the range of 1.1–1.5, and the observed M_n value was consistent with the theoretical molecular weight for the corresponding feed ratios.

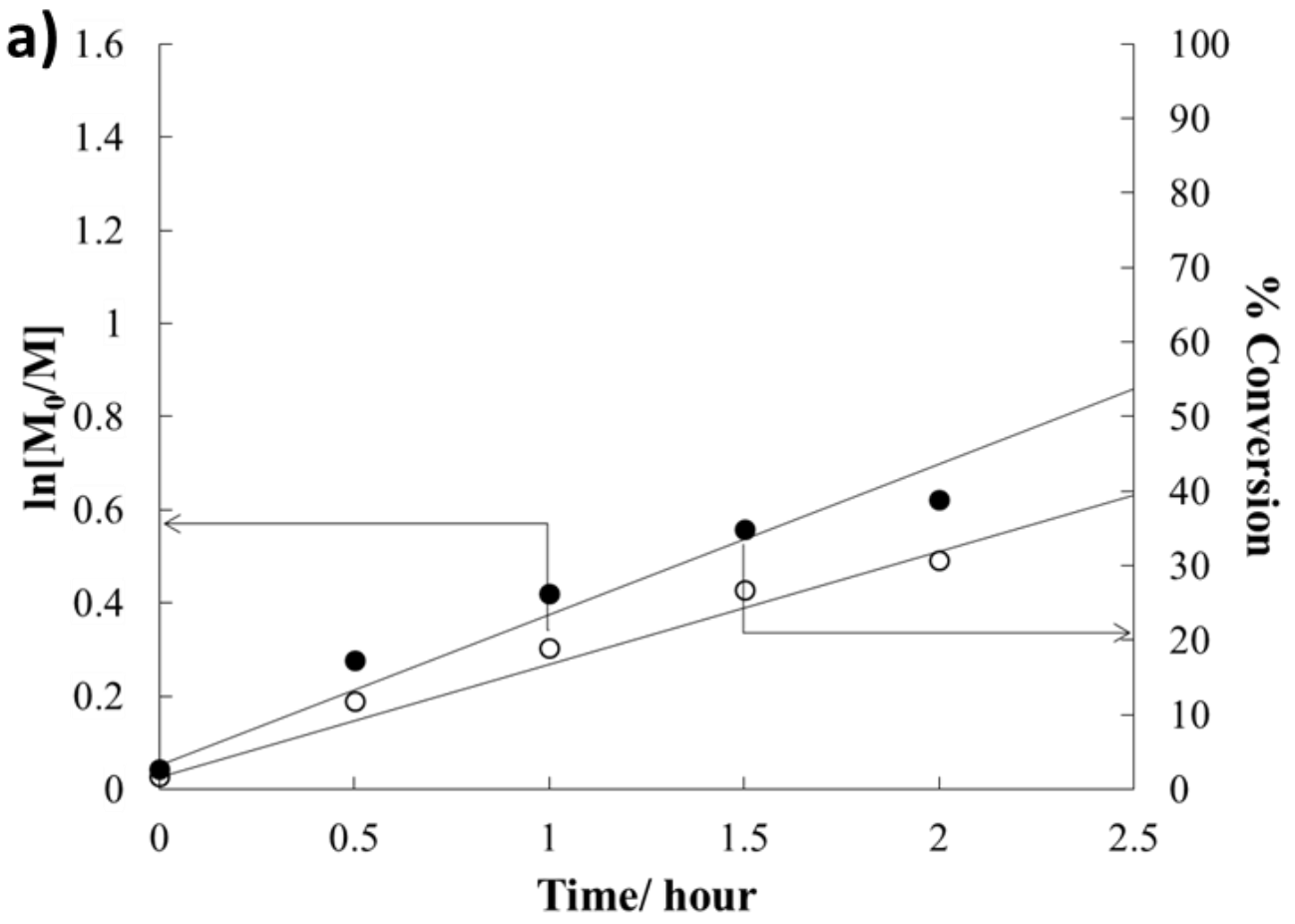
a)
ln[M0/M]
% Conversion
Time/ hour
0
0.2
0.4
0.6
0.8
1
1.2
1.4
1.6
0
10
20
30
40
50
60
70
80
90
100
0
0.5
1
1.5
2
2.5

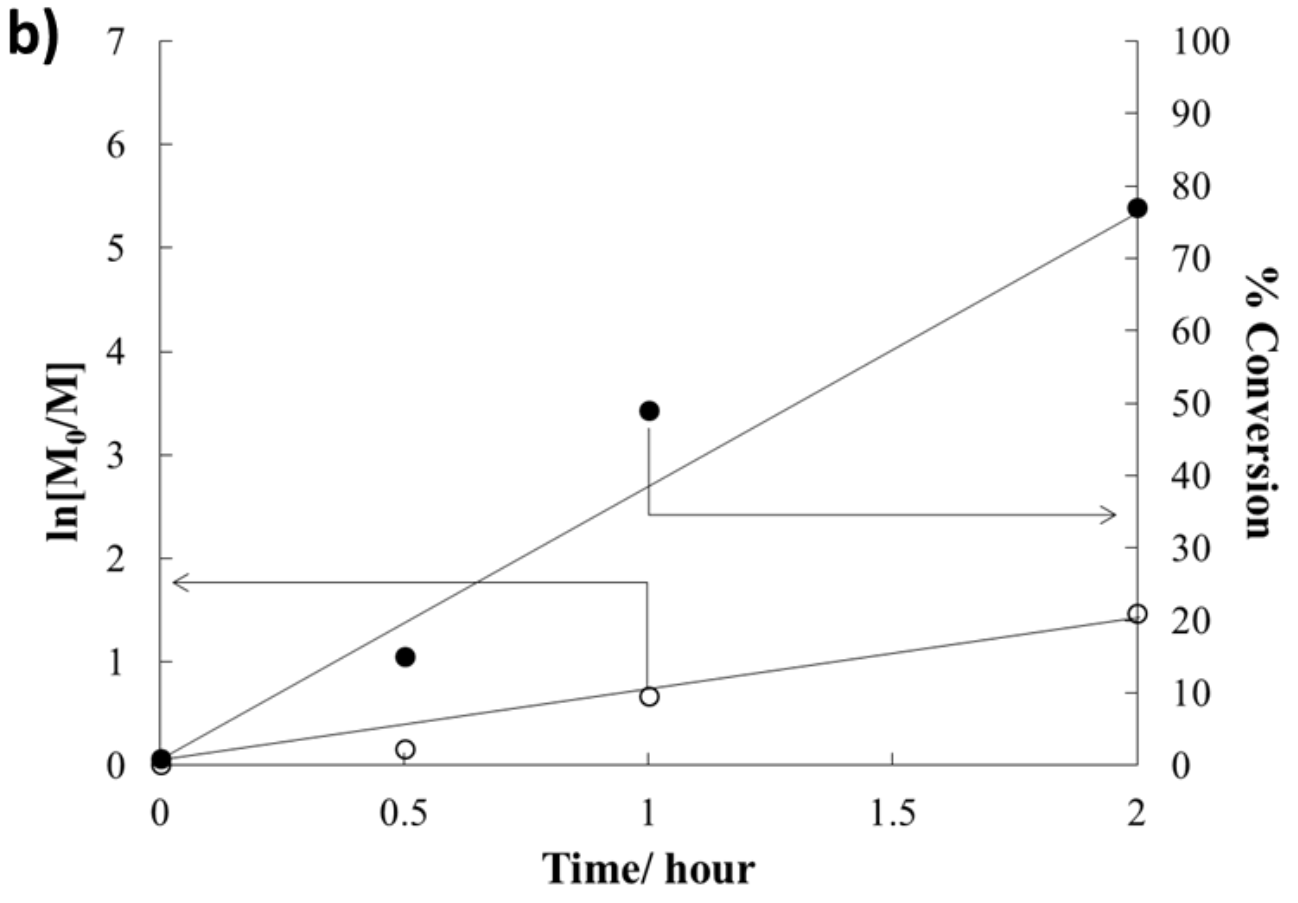
b)
ln[M0/M]
% Conversion
Time/ hour
0
1
2
3
4
5
6
7
0
10
20
30
40
50
60
70
80
90
100
0
0.5
1
1.5
2

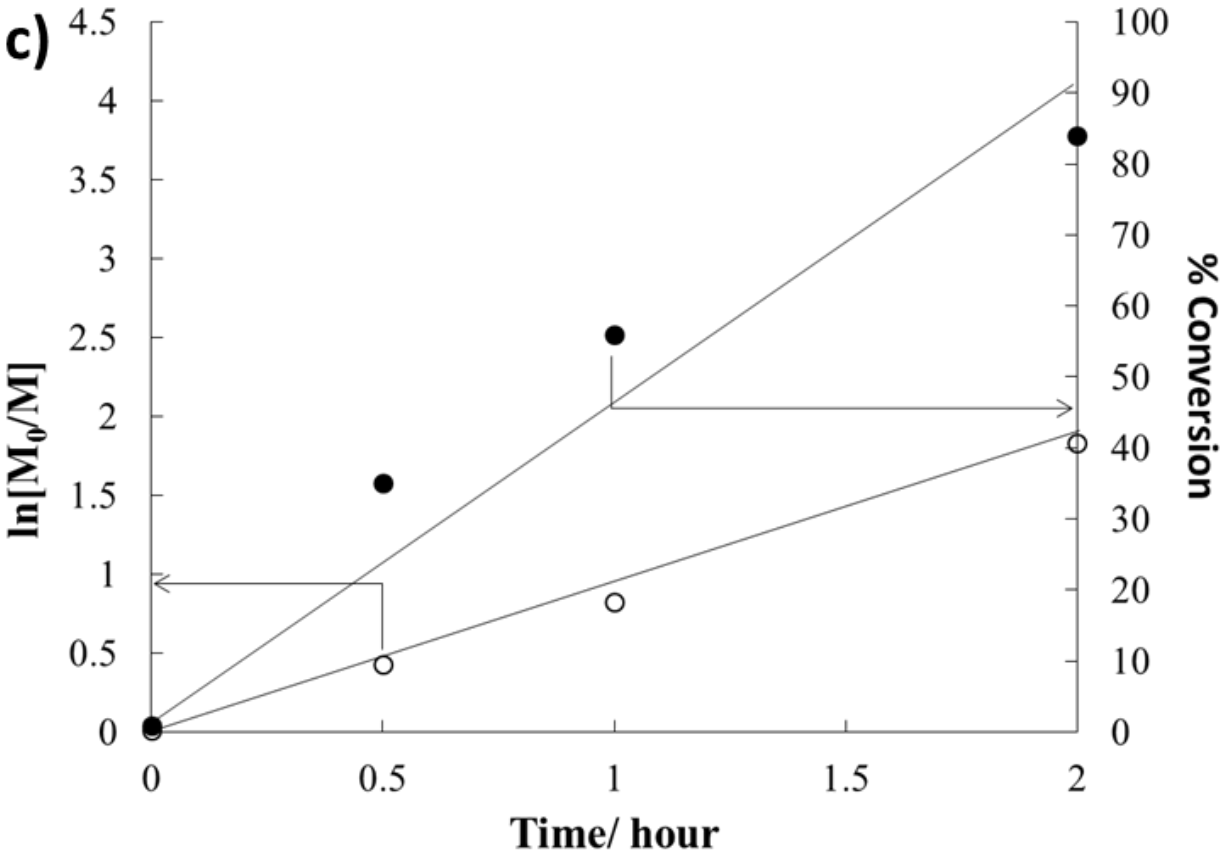

Figure 2. Kinetic plot showing the polymerization of (a) poly-(MAA-DMAEMA), (b) poly-SPB, and (c) poly-CMB by RAFT polymerization, followed by ^{1}H NMR spectroscopy in D_2O

Cryopreservation

L929 cells were cryopreserved with different polymers in DMEM without FBS. Fig. 3 shows the effects of the concentration and hydrophobicity of poly-(MAA-DMAEMA) on the cell viability after cryopreservation. The results unambiguously indicated that poly-(MAA-DMAEMA) has an excellent cryoprotective property, and its efficacy increased with increasing polymer concentrations. Incorporating hydrophobicity into poly-(MAA-DMAEMA) using BuMA or OcMA significantly enhanced the cell viability, which reached 96 % at a 10 % poly-(MAA-DMAEMA) containing 5 % OcMA. The cell viability observed after OcMA substitution was higher than observed following BuMA substitution. This

finding can be explained by the fact that OcMA contains bigger alkyl chain (introducing greater hydrophobicity) than BuMA. These data clearly showed that introducing hydrophobicity into poly-(MAA-DMAEMA) significantly increased cell viability following cryopreservation.

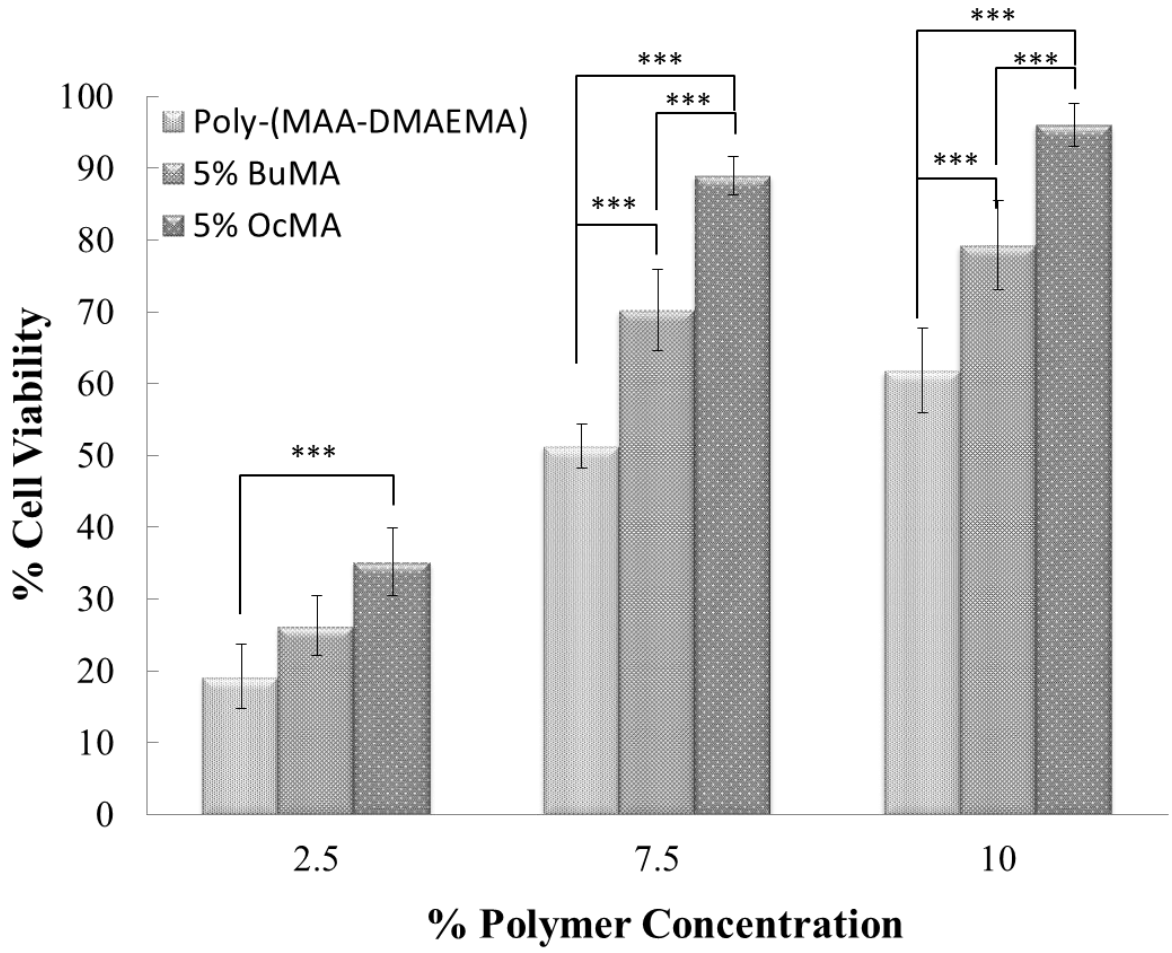

Figure 3. Cryoprotective properties of poly-(MAA-DMAEMA) and the effect of hydrophobicity. L929 cells were cryopreserved with the MAA-DMAEMA copolymer with different polyampholytes at various concentrations. Data are expressed as the mean ± SD for 3 independent experiments (5 samples each). ***P < 0.001

To ascertain the relationship between the polymer structure and the cryoprotective behavior, we developed 2 structurally similar zwitterionic polymers (poly-SPB and poly-CMB) and

compared their cryoprotective properties with that of poly-(MAA-DMAEMA). Fig. 4a shows that poly-SPB conferred less cell viability than did poly-(MAA-DMAEMA), and even at a 15 % concentration, poly-SPB showed only ~65 % cell viability. In contrast, Poly-CMB showed very weak to almost no cryoprotective ability; at a 15 % poly-CMB concentration, only ~4 % viability was observed. These results showed that poly-(MAA-DMAEMA) had exceptionally high cryoprotective ability, whereas poly-SPB showed an intermediate ability, and poly-CMB was ineffective in cryoprotection. Moreover, Fig 4b shows that unlike poly-(MAA-DMAEMA), the introduction of hydrophobicity into poly-SPB and poly-CMB did not have any effect on cell viability. From these results, it was evident that not all polyampholytes possess cryoprotective properties, indicating that the underlying molecular mechanism may depend upon the unique chemical structures of cryoprotectants.

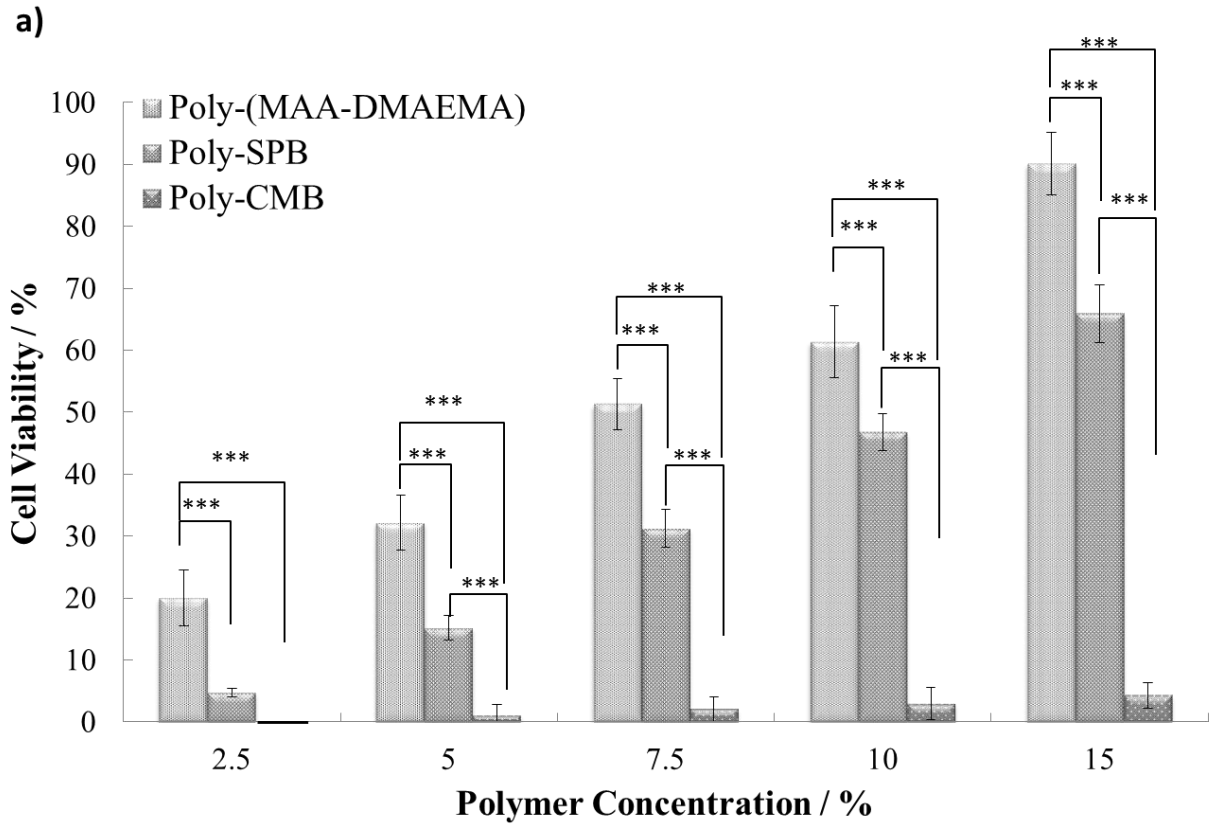

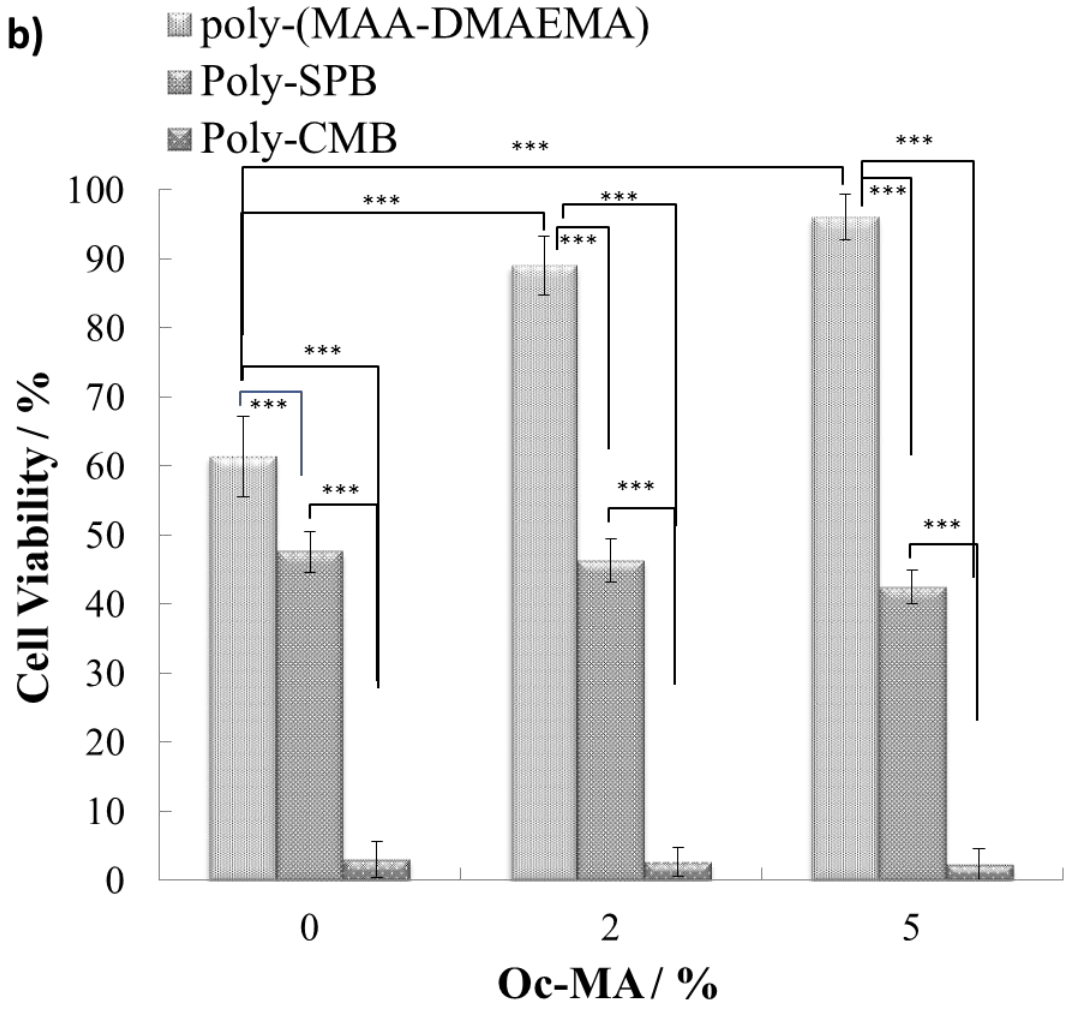

Figure 4. Cryoprotective properties of poly-(MAA-DMAEMA), poly-SPB, and poly-CMB (a) at various polymer concentration or (b) with different OcMA concentrations at a constant 10% polymer concentration. L929 cells were cryopreserved with different polyampholytes at various concentrations. Data are expressed as the mean ± SD for 3 independent experiments (5 samples each). ***P < 0.001

IRI experiments

Ice formation is an undesirable outcome during cryopreservation. Both intracellular and extracellular ice formation are extremely fatal to cells. Extracellular ice formation causes mechanical damage to the cells, as well as osmotic shock resulting from ice formation, which leads to an increased concentration of extracellular solutes.[26] During the freezing process,

small ice crystals are transformed into larger crystals by a process known as ice recrystallization. Recrystallization occurs because smaller ice crystals (which have a greater curvature) tend to have a lower melting point and hence melt at a higher annealing temperature (the Kelvin effect). The released liquid water moves to a neighboring (larger) ice crystal and refreezes, and this new ice crystal will have a higher melting point. In this way, the process of ice recrystallization results in the formation of a matrix composed of larger ice crystals.[27] Ice recrystallization damages cells and tissues during thawing, due to membrane rupture and cell dehydration.[28] Splat cooling assays have been used by metallurgists to measure recrystallization for years, but this technique was first applied to cryobiology by Knight et al.[29] This technique is commonly used to determine the IRI activity of a compound of interest (Fig. 5a). Gibson and his co-workers have performed extensive studies on the IRI activities of polymers, including polyampholytes, and showed that IRI might be related to cryoprotective properties.[19, 24, 30-35]

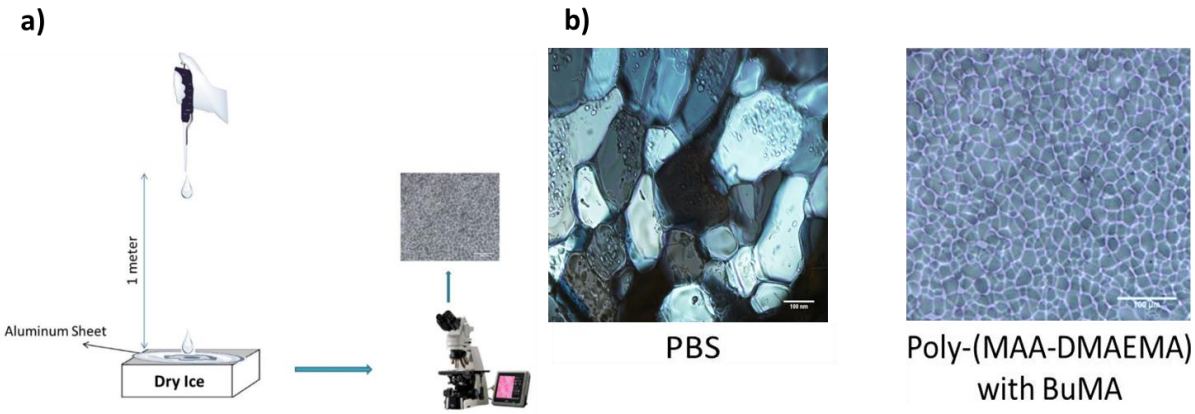

Figure 5. (a) Schematic representation of the splat assay. (b) Micrographs of poly-nucleated ice crystals in PBS alone or in the presence of poly-(MAA-DMAEMA) with BuMA, after a 30-min annealing at –6ºC (scale bars, 100 µm)

In this study, we employed a modified splat assay. Fig. 5b depicts an example of a micrograph of an ice crystal wafer grown in PBS solution alone, as well as a hydrophobic polyampholyte, poly-(MAA-DMAEMA) with 5 % BuMA. With the hydrophobic polymer, the size of the ice crystals was far smaller than when PBS was used.

Fig. 6 shows that all 3 polyampholytes showed IRI activity to a certain degree. This was supported by a previous report by Vorontsov et al., who argued that the polyampholyte COOH-PLL also exhibits an antifreeze property.[36] These authors determined that the antifreeze property was related to the hysteresis of the growth rate and depression of the freezing point. They argued that in the event of ice crystallization, a non-steady-state behavior is displayed during the adsorption of large biological molecules and that its rate is

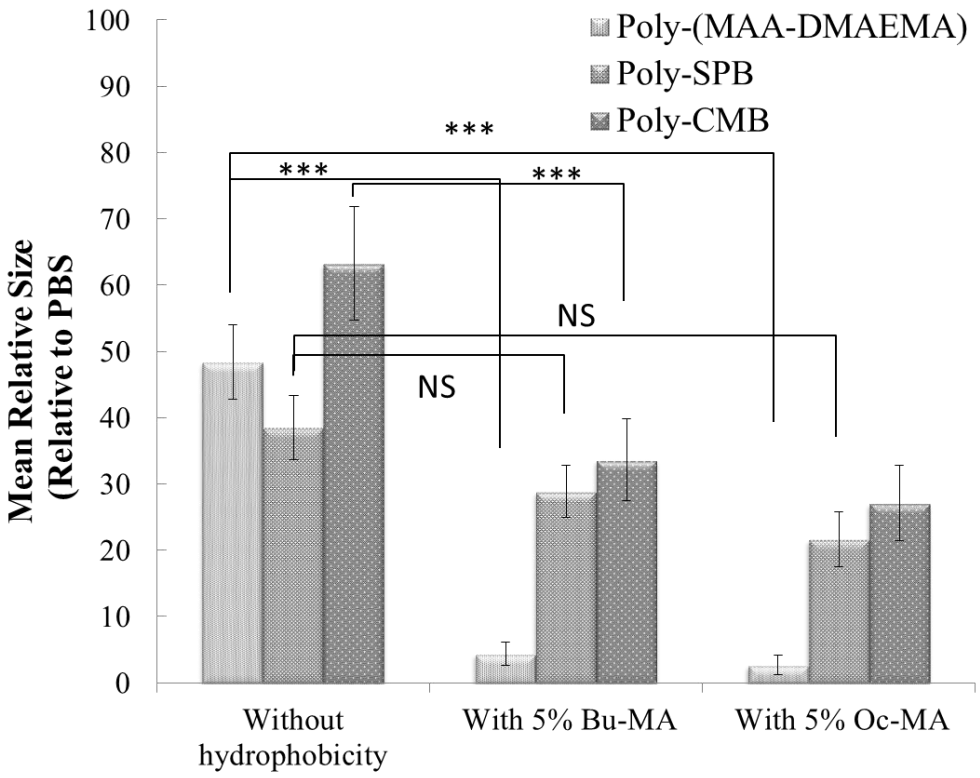

Figure 6. IRI activities of poly-(MAA-DMAEMA), poly-SPB, and poly-CMB and the effect of hydrophobicity at a 10% polymer concentration. The errors bars indicate the SD of the mean. ***P < 0.001, NS: not statistically different

relatively slower than the process of embedding of crystal growth units. However, with the addition of a hydrophobic monomer (BuMA), the size of the ice crystals reduced significantly in the case of poly-(MAA-DMAEMA), whereas no significant differences were observed with poly-CMB and poly-SPB. This is because the introduction of BuMA or OcMA into poly-SPB and poly-CMB did not significantly enhance their hydrophobicity. A previous report by Smith and McCormick reported that hydrophobicity increases with an increase in viscosity in aqueous polymer solutions.[37] Therefore, we performed viscosity measurements (TVE-22; TOKI SANGYO Co., Ltd., Tokyo, Japan) to test this hypothesis (Table S1), which confirmed that even with the addition of BuMA and OcMA, the hydrophobicity did not increase markedly with poly-CMB or poly-SPB. This behavior was corroborated by another report showing that the charge balance of polyampholytes is of the foremost importance and that mixtures with a 1:1 ratio of cationic and anionic moieties showed higher IRI activity. [35] In addition, the authors suggested that mixed-charge side chain polymers have a higher cryoprotection efficacy than do zwitterionic polymers. Increasing the degree of hydrophobicity (by introducing OcMA) led to a further decrease in the size of the crystals, with an MLGS of ~2.6 % found with poly-(MAA-DMAEMA), which implied that this polymer almost completely inhibited ice recrystallization. This finding is supported by evidence from a previous studies showing that IRI activity depends upon the presence of long alkyl chains and increased hydrophobicity.[30, 31, 38, 39] These polymers are believed to act as antifreeze proteins, which bind irreversibly to ice crystals and inhibit their growth.[40] Data from previous studies have shown that the presence of hydrophobic domains in antifreeze glycoproteins with amphipathic character helps to repel additional water molecules, leading to higher activity.[32, 41, 42] Data from another study conducted with a type-III antifreeze protein demonstrated that hydrophobic groups may be involved in the energetics of protein–ice interactions.[32] Findings from Deller et al. showed that synthetic polymers enhanced the

cryopreservation of different cell types by reducing ice-crystal growth during thawing.[43] Thus, we confirmed that the increase in cell viability associated with an increase in hydrophobicity of poly-(MAA-DMAEMA) is linked to its high IRI activity. Poly-CMB by itself did not possess any cryoprotective ability; hence, even with an increase in hydrophobicity, no effect was observed. Therefore, it can be inferred that hydrophobicity only enhances cell viability with polymers that already have some cryoprotective ability. However, when we compared the IRI activity between poly-SPB and poly-CMB (with or without the introduction of hydrophobicity), the values showed similar IRI activities, although the cryoprotective properties were quite different. These results suggested that the IRI activity is an important parameter determining cryoprotective properties, but that other key factors are likely imperative for cryoprotection. It was previously reported that increasing the hydrophobicity in molecules of interest enhanced their cell membrane affinities.[44] Therefore, we investigated the cell membrane interaction of these polymers, based on the hypothesis that cell membrane protection might relate to cryoprotection.

DSC

Liposomes can exist either in a gel state (low temperatures) or in a liquid state (high temperatures). In the gel state, the liposomes are tightly held together by van der Waals forces. Phospholipids cooperatively melt at the phase-transition temperature and transform to the liquid state, where they are more loosely held due to weakened van der Waals interaction between acyl chains.[45] Moreover, lateral expansion of the acyl chains and weaker interactions of polar head groups contribute to the weakened association in the liquid state. Consequently, the gel-liquid crystalline phase-transition temperature is largely due the length of the acyl chain and the nature of phospholipid headgroup.[46]

From the DSC results (Fig. 7), it was established that polyampholytes depressed the bilayer gel-to-liquid crystalline-transition temperature of EPC. Polyampholytes depressed the transition temperature, with increasing polyampholyte concentrations leading to lower transition temperatures. Poly-(MAA-DMAEMA) showed a steep decrease in the phase transition of EPC, with a decrease of >6 °C occurring at a polymer: lipid mass of 0.25 (Fig. S3).

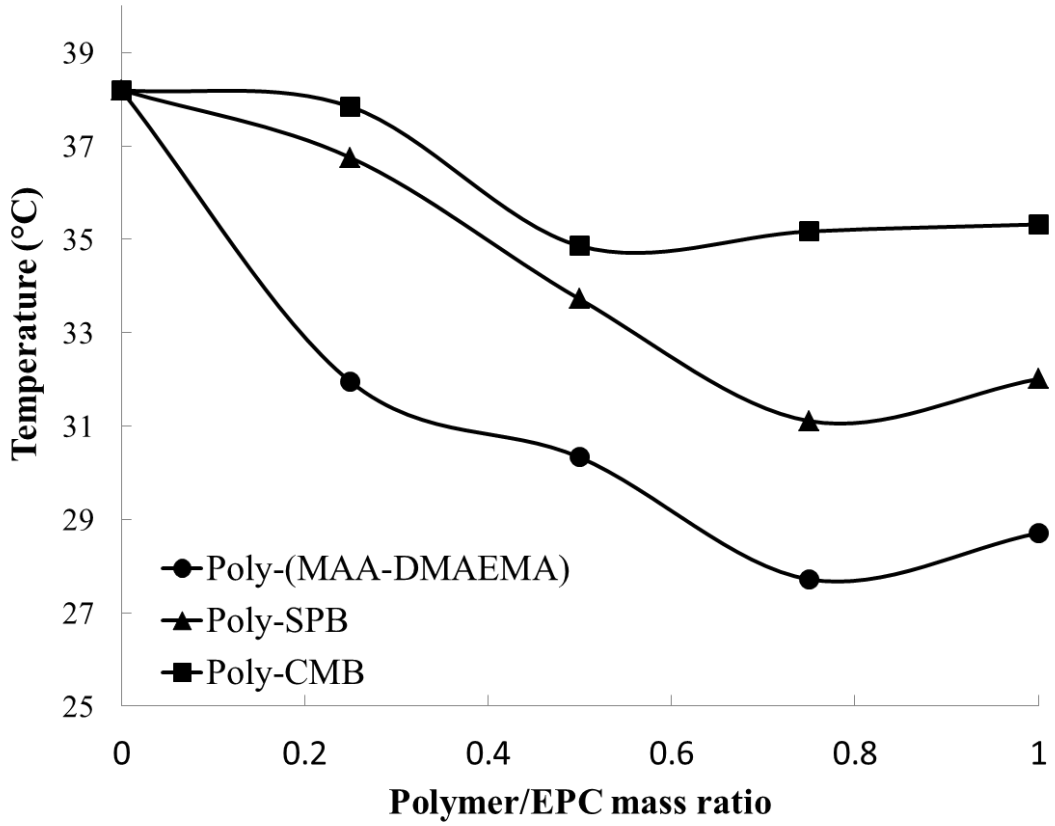

Figure 7. Effects of poly-(MAA-DMAEMA), poly-SPB, and poly-CMB on the gel-to-liquid-crystalline-transition temperature of EPC at polymer/EPC mass ratios between 0 and 1.0

Poly-CMB, however, showed a lesser decrease in the transition temperature. Previous data from Crowe et al. suggested that the establishment of membrane interactions can depress the gel-to-liquid crystalline-phase transition temperature.[47] Thus, our DSC data indicated that poly-(MAA-DMAEMA) has a markedly greater interaction with the cell membrane than does

poly-CMB, and this may be a result of increased spacing between the lipids in the presence of poly-(MAA-DMAEMA), which facilitates a greater number of gauche conformers in the fatty acyl chains.[48] ESR studies were performed to further investigate the interactions between the polyampholytes and membrane in detail.

ESR Spectroscopy

ESR has greater sensitivity than nuclear magnetic resonance (NMR) because of the greater magnetic moment of electrons, compared with that of the nucleus. ESR can be used to study fast dynamics. Biological systems (including membranes) lack unpaired electrons, so they cannot be investigated by ESR in their native states.[49] This limitation was overcome by spin labeling the membranes by the incorporation of spin-bearing probes.

The effect of polyampholytes on the polar region of the membrane during freezing was investigated by conducting ESR studies with freeze-thawed 5-DSA liposomes supplemented with polymers of different concentrations. Fig. 8a shows that poly-(MAA-DMAEMA) interacts with the outer surface of the membrane, as indicated by a significant decrease in the order parameter. Poly-SPB also showed a similar effect, with a considerable interaction with the membrane surface. However, poly-CMB did not exhibit a large decrease in the order parameter value, signifying a low interaction with the cell membrane (Fig. 8b). Poly-(MAA-DMAEMA) interactions may results from an electrostatic association with the membrane. In contrast, with poly-CMB and poly-SPB, the major difference lies in the basicity of the polymer, with carboxylate group in poly-CMB being a stronger than that of the sulfonate group of poly-SPB and as such, the carboxylate group in poly-CMB becomes non-ionic by lowering the pH.[50, 51] Therefore, poly-SPB interacts strongly with the membrane electrostatically, whereas poly-CMB does not. The ESR spectrum of the hydrophobic

derivative of poly-(MAA-DMAEMA) showed a lower interaction due to the effect of the hydrophobic moieties.

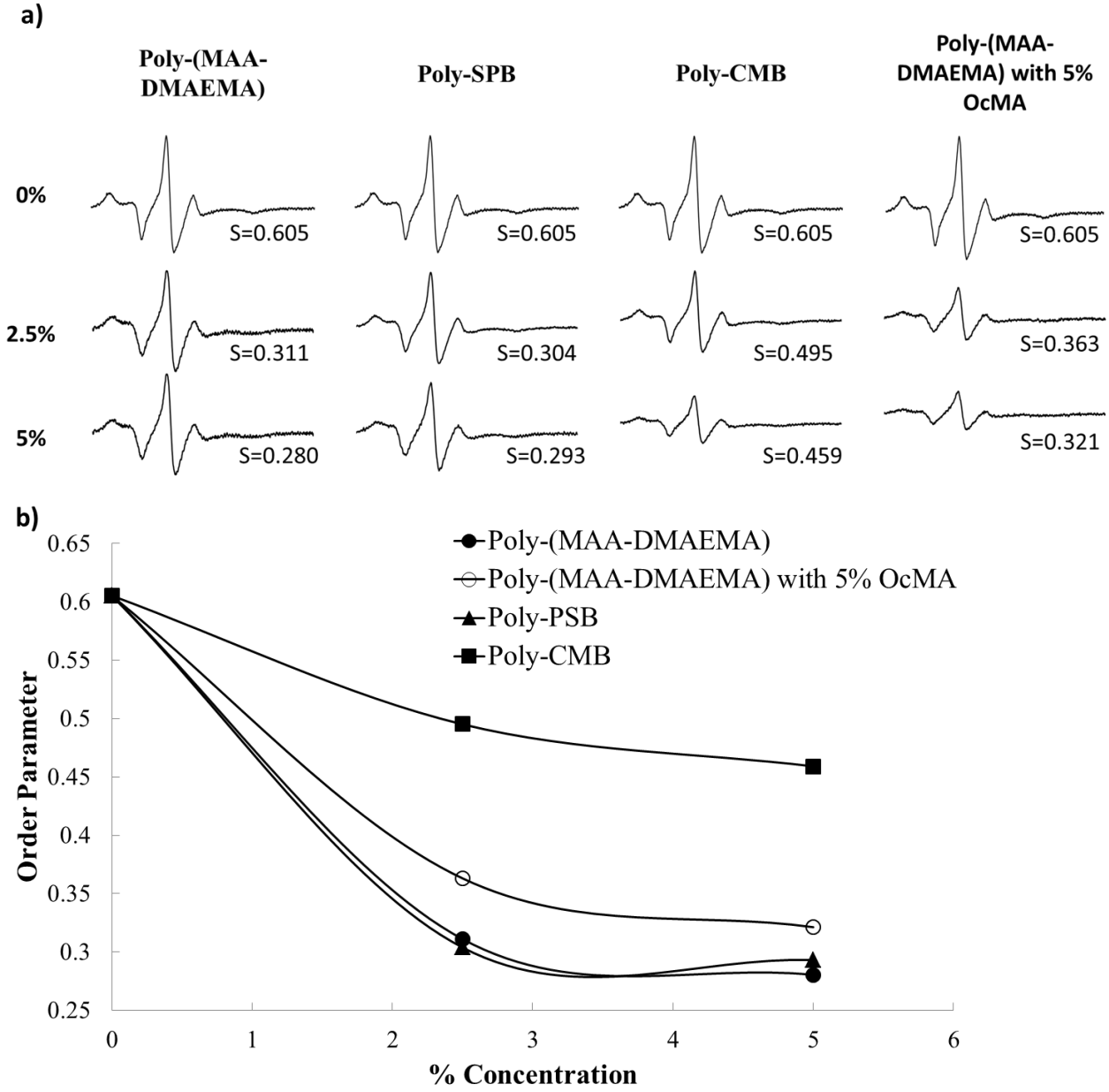

Figure 8. (a) ESR spectra of 5-DSA (1 mol%) incorporated into EPC in the presence of various polymers at different polymer concentrations. The numbers shown denote the order parameter (S). (b) The polyampholyte concentration dependence of the order parameter S for 5-DSA (1 mol %) intercalated into unilamellar dispersions of EPC in PBS buffer (pH 7.4).

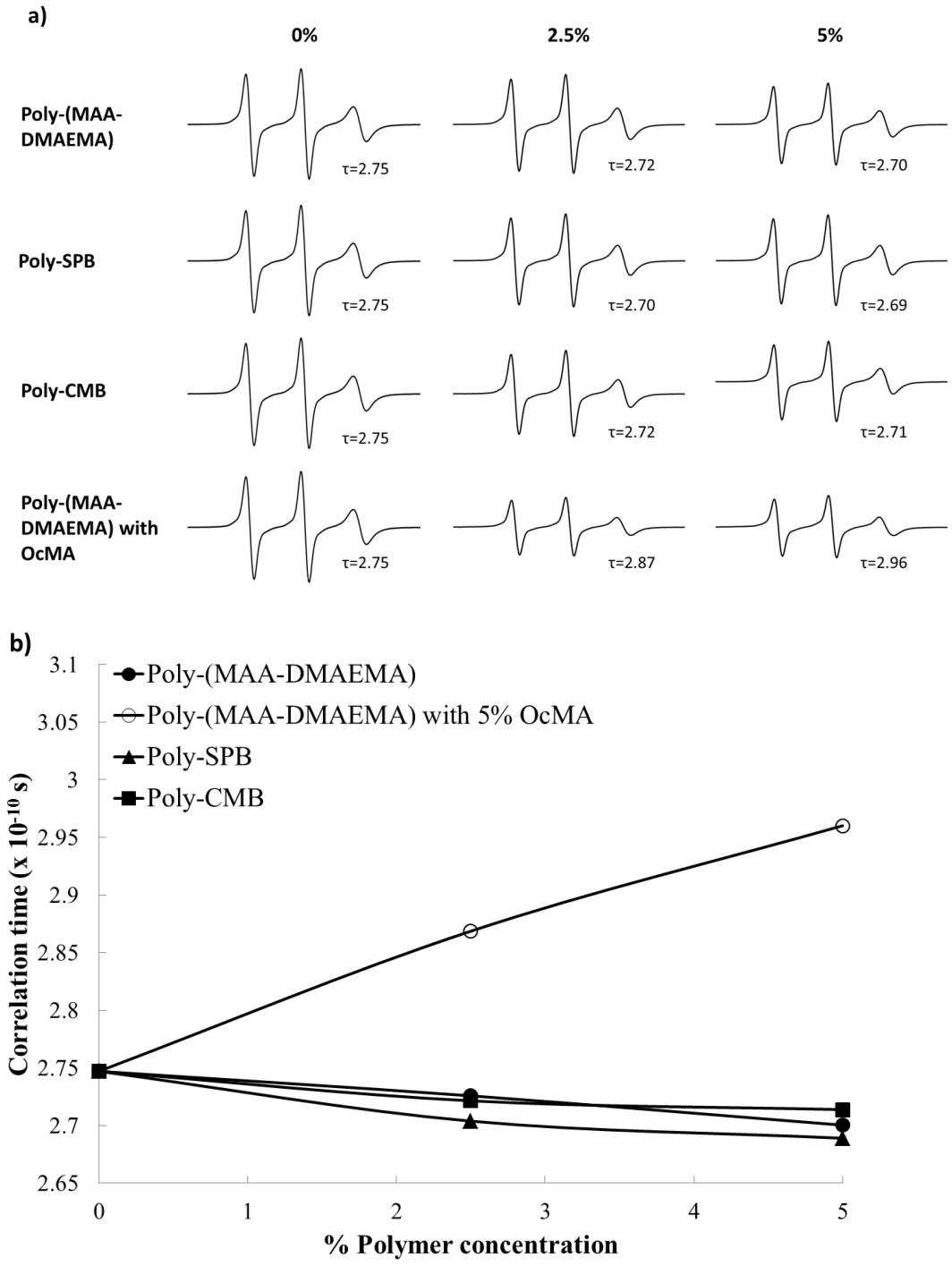

Figure 9. (a) ESR spectra of 16-DSA (1 mol %) intercalated into EPC in the presence of various polymers at different polymer concentrations. The numbers shown denote the correlation time (τ). (b) The polyampholyte concentration dependence of correlation time τ for 16-DSA (1 mol %) intercalated into unilamellar dispersions of EPC in PBS buffer (pH 7.4)

Incorporation of 16-DSA into the membrane showed that none of the 3 polymers interacted with the hydrophobic region of the membrane, which is represented by almost no change in the correlation time (Fig. 9a). This finding indicated that these polymers are not present in this region. However, poly-(MAA-DMAEMA) with 5 % OcMA exhibited an increase in the correlation time (Fig. 9b), implying that this polymer showed a significant interaction with the probe, which was present in the hydrophobic core of the membrane. This finding could be attributed to its penetration or localization in this region. This possibility is supported by previous data revealing that hydrophobic drugs penetrate the cell membrane, whereas their hydrophilic counterparts do not.[52-55] Similar observations were obtained where tocopheryl polyethylene glycol succinate-coated poly(D,L-lactide-co-glycolide) nanoparticles showed greater penetration into the dipalmitoylphosphatidylcholine lipid membrane than did polyvinyl alcohol-coated poly(D,L-lactide-coglycolide).[56] Data from another study performed with polyampholytes revealed that introducing hydrophobicity to polyampholytes facilitated their adsorption onto the cell membrane and subsequent penetration.[57] Investigation of the change in correlation time with respect to different hydrophobic polyampholytes was also performed. Fig. 10 shows that a hydrophobic derivative of poly-(MAA-DMAEMA) caused the maximum deviation in correlation time values, whereas only marginal changes were observed in the case of poly-SPB. This finding could be attributed to the relatively high water solubility (hydrophilicity) observed in poly-SPB with 5 % OcMA when compared to the corresponding hydrophobic poly-(MAA-DMAEMA). Poly-CMB with 5 % OcMA showed almost no change in the correlation time value, which is also attributable to the low hydrophobicity of the BuMA and OcMA derivatives of poly-SPB and poly-CMB (Table S1).

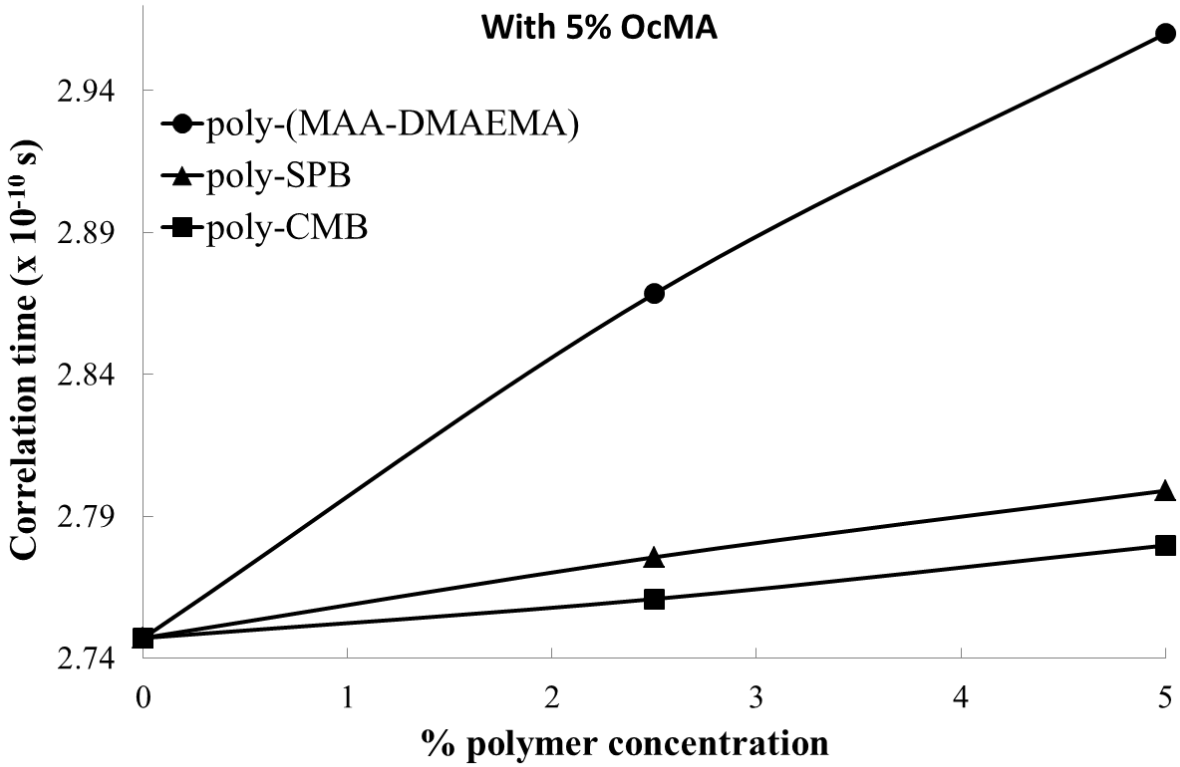

Figure 10. Concentration dependence of hydrophobic polyampholytes (with 5% OcMA) on the correlation time τ for 16-DSA (1 mol %) intercalated into unilamellar dispersions of EPC in PBS buffer (pH 7.4)

A schematic representation of the localization of different polyampholytes around the cell membrane is presented in Fig. 11. Poly-SPB is present near the polar (hydrophilic) head region of the membrane. This is supported by the fact that a large decrease in the order parameter of 5-DSA in the lipid bilayer was observed in the presence of poly-SPB. Apart from the electrostatic interaction, this may also be due to its high hydrophilicity. Poly-(MAA-DMAEMA) is also located near the polar region, as suggested by a decrease in the order parameter, but is positioned slightly lower than poly-SPB, owing to its higher relative hydrophobicity. This possibility is also supported by the observation that the hydrophobic derivative poly-SPB disturbs the correlation time to a greater extent than poly-SPB. In contrast, poly-(MAA-DMAEMA) with OcMA becomes localized near the hydrophobic tail of the lipid membrane.

Data from the DSC, ESR, and IRI studies established that cryoprotective polymers showed greater interactions with the cell membrane. This interaction might protect the membrane from various freezing-induced damages, such as physical (mechanical) damage resulting from ice recrystallization and chemical osmotic damages.

After confirming that cryoprotective polymers interact more strongly with the cell membrane and that this interaction is cryoprotective in nature, we validated this finding by quantitatively analyzing membrane damage after freezing in presence of different polymers.

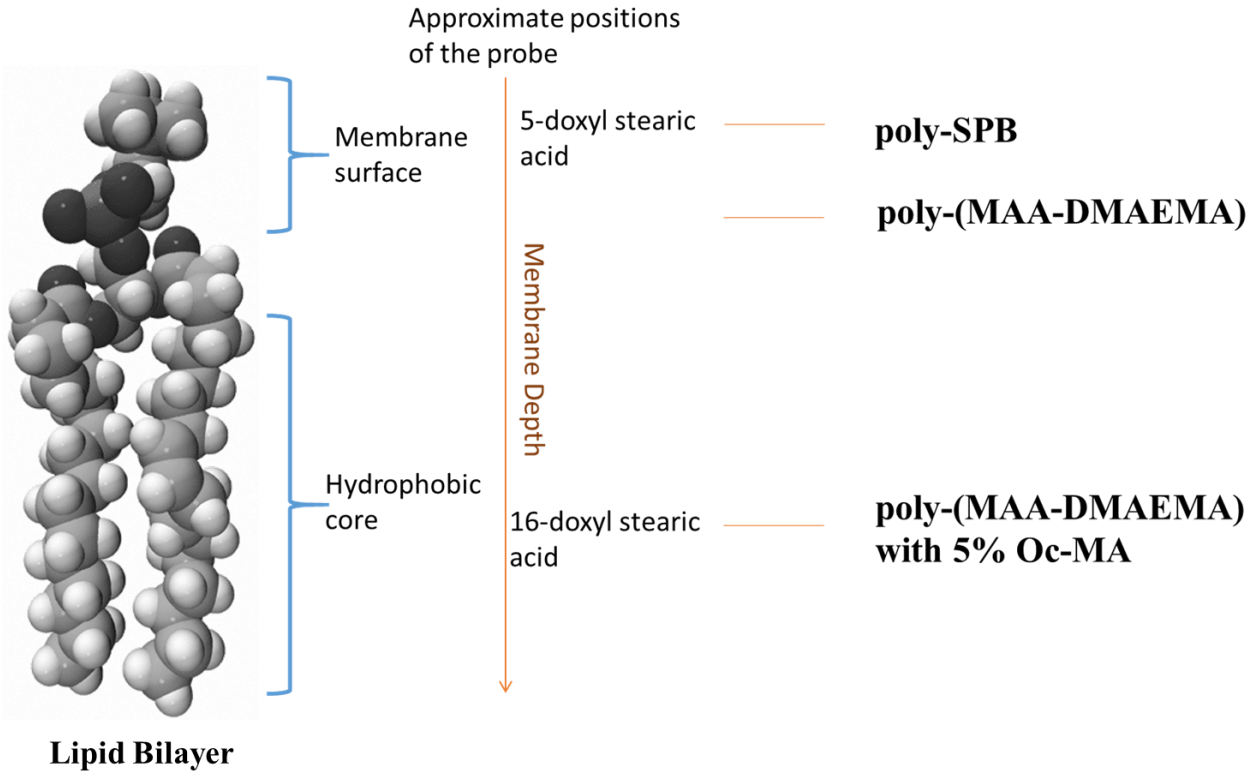

Figure 11. Schematic representation of membrane-polyampholyte interaction/localization

Leakage Experiment

Fig. 12 shows that when no polyampholytes were added to the liposomes, maximum leakage was observed, due to membrane damage/lysis that resulted in the release of the soluble marker (CF) enclosed in the liposome to the surrounding buffer. The leakage began to

decrease upon the addition of poly-(MAA-DMAEMA) and at 10 %, only ~35 % leakage was observed. This finding indicated that this polymer protected the membrane during the freeze-thaw process and that cryoprotection increased with an increasing polymer concentration. This in in good agreement with the cryopreservation results obtained using the same polymer. However, the presence of poly-SPB also reduced membrane leakage, but the extent of membrane protection was lesser than that of poly-(MAA-DMAEMA). These findings corresponded well with the cryopreservation results. Poly-CMB only marginally inhibited leakage, and no significant change was observed even with increasing polymer concentrations. These data showed that poly-(MAA-DMAEMA) conferred the greatest membrane protection, followed by poly-SPB, and then by poly-CMB, which did not exhibit membrane-protection ability. These findings can explain the differences in the cryopreservation properties of different polyampholytes.

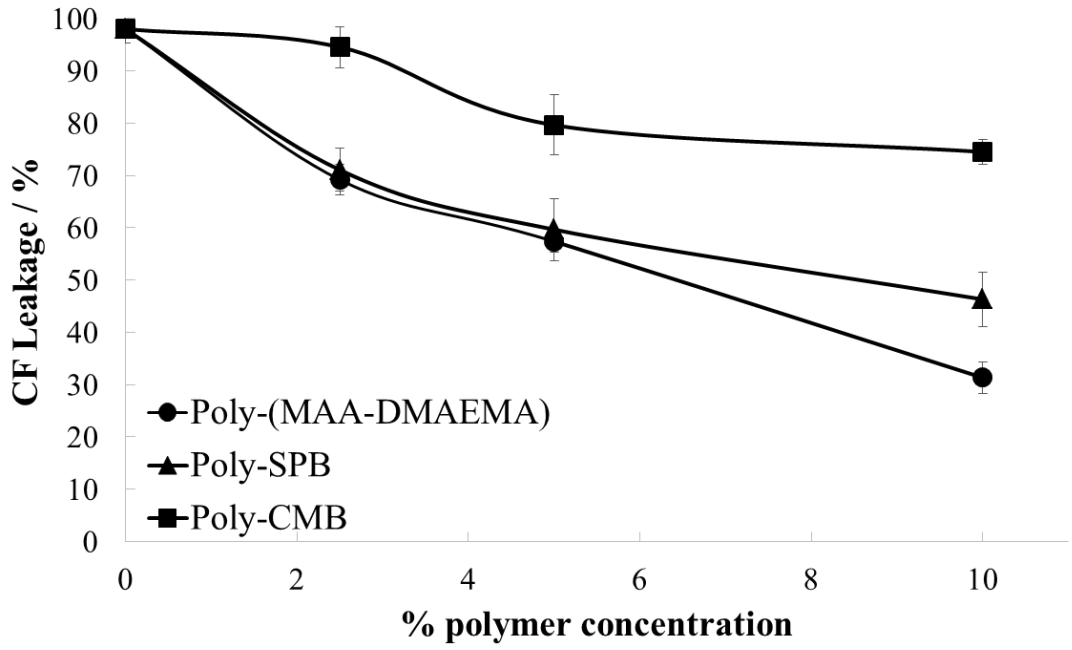

Figure 12. Protection of liposomes during freezing by different polyampholytes. CF leakage from liposomes cryopreserved with various polyampholytes solutions at different polymer concentrations. Data are expressed as the mean ± SD for 3 independent experiments (5 samples each).

CONCLUSION

In this study, we demonstrated that synthetic polyampholytes can behave as excellent cryoprotective agents for cells, whose potential can be further augmented by supplementing the polyampholytes with a small degree of hydrophobicity. Moreover, we established that the mere presence of both positive and negative charges in a polymer is insufficient for cryoprotection and that the polymer structure influences its activity. This was indicated by the disparate cryoprotective properties shown by different polyampholytes, which was due to the differing interactions of different polymers with the cell membrane. Polymers showing the higher cryoprotective properties also showed a greater interaction with the cell membrane, which was evident from a depression in the phase-transition temperature of the membrane and a greater polymer penetration inside the membrane. Membrane protection by cryoprotective polymers was further validated by demonstrating the greater IRI activities during freezing, which is important because IRI is one of the primary reasons for membrane damage during cryopreservation. Hydrophobicity further enhanced the IRI activity. Leakage experiments confirmed that membrane protection during freezing directly affects the cryopreservation ability, with more cryoprotective polymers showing greater membrane protection. Finally, the results showed that synthetic polyampholytes can be fine-tuned to be excellent CPAs, where polymer structure and functionality determines their cryoprotective ability. Polymers cryopreserve cells by a synergistic effect involving numerous parameters. The data presented in this study shed insight into the mechanism of cryopreservation, which should enable the more efficient molecular design of CPAs in the future. Further studies are warranted to understand the dynamics and molecular events involved in membrane protection during freezing, through studies such as molecular simulations. Additionally, study of interaction of polymers with transmembrane proteins and lipids could enable a comprehensive understanding of the mechanism.

ASSOCIATED CONTENT

Supporting Information.

The Supporting Information is available free of charge on the ACS Publications website at DOI:

Time dependent NMR of the 3 polyampholytes (Figure S1); 2D NMR for polymer characterization (Figure S2); DSC heating thermograms of liposomes in the presence of different polyampholytes (Figure S3); viscosity measurements of polyampholytes with BuMA or OcMA (Table S1)

AUTHOR INFORMATION

Corresponding Author

Kazuaki Matsumura

School of Materials Science, Japan Advanced Institute of Science and Technology, 1-1 Asahidai, Nomi, Ishikawa 923-1292, Japan

E-mail address: mkazuaki@jaist.ac.jp

Tel.: +81-761-51-1680

Fax: +81-761-51-1149

Author contributions

The manuscript was written through contributions of all authors. All authors have given approval to the final version of the manuscript.

Funding Sources

This study was supported in part by a Grant-in-Aid, KAKENHI (25242050), for Scientific Research from the Ministry of Education, Culture, Sports, Science and Technology, Japan and a Collaborative Research Project organized by the Interuniversity Bio-Backup Project (IBBP).

REFERENCES

1. Polge, C.; Smith, A. U.; Parkes, A. S. *Nature* **1949**, 164, 666.
2. Lovelock, J. E.; Bishop, M. W. *Nature* **1959**, 183, 1394–1395.
3. Karlsson, J. O. M.; Toner, M. *Biomaterials* **1996**, 17, 243-256.
4. Lynch, M. E.; Diller, K. R. *Trans. ASME* **1981**, 81, 229-232.
5. Mazur, P. *J. Gen. Physiol.* **1963**, 47, 347-369.
6. Gao, D.; Critser, J. K. *ILAR J.* **2000**, 41, 187-196
7. Woelders, H.; Matthijs, A.; Engel, B. *Cryobiology* **1997**, 35, 93–105.
8. Mazur, P.; Leibo, S.; Farrant, J.; Chu, E.; Hanna, M.; Smith, L. Interactions of cooling rate, warming rate and protective additive on the survival of frozen mammalian cells. *In Ciba Foundation Symposium - The Frozen Cell*; Wolstenholme G. E. W., O′ Connor M, Eds.; John Wiley & Sons, Ltd.: Chichester, UK, 2008, pp 69-88.
9. Pegg, D. E.; Diaper, M. P. *Biophys. J.* **1988**, 54, 471–488.
10. Fahy, G. M. *Cryobiology* **1986**, 23, 1–13.
11. Oh, J. E.; Raja, K. K.; Shin J. H.; Pollak, A.; Hengstschlager, M.; Lubec, G. *Amino Acids* **2006**, 31, 289–298.
12. Matsumura, K., Hyon, S. H. *Biomaterials* **2009**, 30, 4842-4849.
13. Matsumura, K., Bae, J. Y.; Hyon, S. H. *Cell Transplant.* **2010**, 19, 691-699.
14. Jain, M.; Rajan, R.; Hyon, S. H.; Matsumura, K. *Biomater. Sci.* **2014**, 2, 308-317.
15. Kudaibergenov, S. E. Applications of polyampholytes. In *Polyampholytes synthesis, characterization, and application*; Springer: New York, 2002, pp 189-202.
16. Rajan, R.; Matsumura, K. *J. Mater. Chem. B* **2015**, 3, 5647-5894.
17. Laughlin, R. G. *Langmuir* **1991**, 7, 842–847.
18. Rajan, R.; Jain, M.; Matsumura, K. *J. Biomater. Sci., Polym. Ed.* **2013**, 24, 1767-1780.

19. Mitchell, D. E.; Cameron, N. R.; Gibson, M. I. *Chem. Commun.* **2015**, 51, 12977-12980.
20. Lai, C.-S.; Schutzbach, J. S. *FEBS Lett.* **1986**, 203, 153-156.
21. Wassall, S. R.; Phelps, T. M.; Albrecht, M. R.; Langsford C. A.; Stillwell, W. *Biochim. Biophys. Acta, Biomembr.* **1988**, 939, 393-402.
22. Yin, J. J.; Smith, M. J.; Eppley, R. M.; Page, S. W.; Sphon, J. A.; Biochim. *Biophys. Acta, Biomembr.* **1998**, 1371, 134-142.
23. Štrancar, J. In ESR Spectroscopy in Membrane Biophysics; Hemminga, M. A., Berliner, L. J., Eds.; Springer Science: New York, **2007**; Chapter 3, 49−93.
24. Gibson, M. I. *Polym. Chem.* **2010**, 1, 1141−1152.
25. Kitano, H.; Kondo, T.; Kamada, T.; Iwanaga, S.; Nakamura, M.; Ohno, K. *Colloids Surf., B* **2011**, 88, 455–462.
26. Mazur, P. *Am. J. Physiol.* **1984**, 247, C125-C142.
27. Knight, C. A.; Duman, J. G. *Cryobiology* **1986**, 23, 256-262.
28. Zalis, S.; Dolev, M. B.; Braslavsky, I. *Cryobiology* **2013**, 67, 438.
29. Knight, C. A.; Hallett, J.; Vries, A. L. D. *Cryobiology* **1988**, 25, 55-60.
30. Congdon, T.; Notman, R.; Gibson, M. I. *Biomacromolecules* **2013**, 14, 1578−1586.
31. Deller, R. C.; Congdon, T.; Sahid, M. A.; Morgan, M.; Vatish, M.; Mitchell, D. A.; Notman, R.; Gibson, M. I. *Biomater. Sci.* **2013**,1, 478-485.
32. Deller, R. C.; Vatish, M.; Mitchell, D. A.; Gibson, M. I. *Nat. Commun.* **2014**, 5, 3244.
33. Deller, R. C.; Vatish, M.; Mitchell, D. A.; Gibson, M. I. *ACS Biomater. Sci. Eng.* **2015**, 1, 789−794.
34. Congdon, T.; Dean, B. T.; Wright, J. K.; Biggs, C. I.; Notman, R.; Gibson, M. I. *Biomacromolecules* **2015**, 16, 2820-2826.

35. Mitchell, D. E.; Lilliman, M.; Spain, S. G.; Gibson, M. I. *Biomater. Sci.* **2014**, 2, 1787-1795.

36. Vorontsov, D. A.; Sazaki, G.; Hyon, S. H.; Matsumura, K.; Furukawa, Y. *J. Phys. Chem. B* **2014**, 118, 10240–10249.

37. Smith, G. L.; McCormick, C. L. *Macromolecules* **2001**, 34, 918-924.

38. Capicciotti, C. J.; Leclere, M.; Perras, F. A.; Bryce, D. L.; Paulin, H.; Harden, J.; Liu, Y.; Ben, R. N. *Chem. Sci.* **2012**, 3, 1408-1416.

39. Balcerzak, A. K.; Febbraro, M.; Ben, R. N. *RSC Adv.* **2013**, 3, 3232-3236.

40. Raymond, J.A.; DeVries, A.L. *Proc. Natl. Acad. Sci. U. S. A.* **1977**, 74, 2589–2593.

41. Tachibana, Y.; Fletcher, G. L.; Fujitani, N.; Tsuda, S.; Monde, K.; Nishimura, S.-I. *Angew. Chem., Int. Ed.* **2004**, 43, 856−862.

42. Garnham, C. P.; Campbell, R. L.; Davies, P. L. *Proc. Natl. Acad. Sci. U. S. A.* **2011**, 108, 7363−7367.

43. Sönnichsen, F. D.; DeLuca, C. I.; Davies, P. L.; Sykes, B. D. *Structure*, **1996**, 4, 1325–1337.

44. Ijäs, H. K.; Lönnfors, M.; Nyholm, T. K. M. *Biochim. Biophys. Acta, Biomembr.* **2013**, 1828, 932–937.

45. Chapman, D. *Q. Rev. Biophys.* **1975**, 8, 185-235.

46. Szoka, F.; Papahadjopoulos, D. *Annu. Rev. Biophys. Bioeng*, **1980**, 9, 467-508.

47. Crowe, J. H.; Hoekstra, F. A.; Crowe, L. M. *Annu. Rev. Physiol.* **1992**, 54, 579-599.

48. Cacela, C.; Hincha, D. K. *Biophys. J.* **2006**, 90, 2831–2842.

49. Borbat, P. P.; Costa-Filho, A. J.; Earle, K. A.; Moscicki, J. K.; Freed, J. H. *Science* **2001**, 291, 266-269.

50. Kathmann, E. E.; McCormick, C. L. *J. Polym. Sci., Part A: Polym. Chem.* **1997**, 35, 231-242.

51. Kathmann, E. E.; McCormick, C. L. *J. Polym. Sci., Part A: Polym. Chem.* **2000**, 35, 243-253.

52. Levin, V.A. *J. Med. Chem.* **1980**, 23, 682–684.

53. Bradbury, M. W. B. *Circ. Res.* **1985**, 57, 213–222.

54. Cefalu, W. T.; Pardridge, W. M. *J. Neurochem.* **1985**, 45, 1954–1956.

55. Seelig, A.; Gottschlich, R.; Devant, R.M. *Proc. Natl. Acad. Sci. U. S. A.* **1994**, 91, 68–72.

56. Mu, L.; Seow, P. H. *Colloids Surf., B* **2006**, 47, 90–97.

57. Ahmed, S.; Hayashi, F.; Nagashima, T.; Matsumura, K. *Biomaterials* **2014**, 35, 6508-6518.

Table 1. Characteristics of various polyampholytes prepared via RAFT polymerization. a) Determined by ^{1}H-NMR, b) [monomer]:[initiator]:[RAFT agent]

Entry		Composition				Molar ratio[b]	$M_n \times 10^{-3}$, [c]	M_w/M_n[c]
		DMAEMA	MAA	Bu-Ma	Oc-Ma			
1	In Feed	50	50	0	0	100:1:5	4.8	1.21
	In Polymer[a)]	50.3	49.7	0	0			
2	In Feed	49	49	2	0	102:1:5	4.9	1.32
	In Polymer[a)]	49.3	48.7	2.0	0			
3	In Feed	47.5	47.5	5	0	105:1:5	5.05	1.36
	In Polymer[a)]	47.7	47.3	5.0	0			
4	In Feed	49	49	0	2	102:1:5	4.95	1.23
	In Polymer[a)]	49.4	48.6	0	2.0			
5	In Feed	47.5	47.5	0	5	105:1:5	5.36	1.32
	In Polymer[a)]	47.6	47.5	0	4.9			

Entry		Composition				Molar ratio[b]	$M_n \times 10^{-3}$, [c]	M_w/M_n[c]
		SPB	CMB	Bu-Ma	Oc-Ma			
6	In Feed	100	0	0	0	100:1:5	5.5	1.18
	In Polymer[a)]	100	0	0	0			
7	In Feed	98	0	2	0	102:1:5	5.7	1.29
	In Polymer[a)]	98.6	0	1.4	0			
8	In Feed	95	0	5	0	105:1:5	6.0	1.42
	In Polymer[a)]	96.1	0	3.9	0			
9	In Feed	98	0	0	2	102:1:5	5.7	1.34
	In Polymer[a)]	98.3	0	0	1.7			
10	In Feed	95	0	0	5	105:1:5	6.1	1.37
	In Polymer[a)]	95.9	0	0	4.1			
11	In Feed	0	100	0	0	100:1:5	4.1	1.32
	In Polymer[a)]	0	100	0	0			
12	In Feed	0	98	2	0	102:1:5	4.3	1.44
	In Polymer[a)]	0	98.4	1.6	0			
13	In Feed	0	95	5	0	105:1:5	4.6	1.39
	In Polymer[a)]	0	96	4	0			
14	In Feed	0	98	0	2	102:1:5	4.4	1.41
	In Polymer[a)]	0	98.3	0	1.7			
15	In Feed	0	95	0	5	105:1:5	4.6	1.49
	In Polymer[a)]	0	95.9	0	4.1			

Figure Captions

Scheme 1. Synthesis of (a) poly-(MAA and DMAEMA) (b) poly-SPB, (c) poly-CMB, and (d) hydrophobic derivatives of polyampholytes by RAFT polymerization

Figure 1. ESR spectra of (a) 5-DSA and (b) 16-DSA in EPC liposomes in PBS (pH 7.4)

Figure 2. Kinetic plot showing the polymerization of (a) poly-(MAA-DMAEMA), (b) poly-SPB, and (c) poly-CMB by RAFT polymerization, followed by ^{1}H NMR spectroscopy in D_2O

Figure 3. Cryoprotective properties of poly-(MAA-DMAEMA) and the effect of hydrophobicity. L929 cells were cryopreserved with the MAA-DMAEMA copolymer with different polyampholytes at various concentrations. Data are expressed as the mean ± SD for 3 independent experiments (5 samples each). ***P < 0.001

Figure 4. Cryoprotective properties of poly-(MAA-DMAEMA), poly-SPB, and poly-CMB (a) at various polymer concentration or (b) with different OcMA concentrations at a constant 10% polymer concentration. L929 cells were cryopreserved with different polyampholytes at various concentrations. Data are expressed as the mean ± SD for 3 independent experiments (5 samples each). ***P < 0.001

Figure 5. (a) Schematic representation of the splat assay. (b) Micrographs of poly-nucleated ice crystals in PBS alone or in the presence of poly-(MAA-DMAEMA) with BuMA, after a 30-min annealing at −6ºC (scale bars, 100 μm)

Figure 6. IRI activities of poly-(MAA-DMAEMA), poly-SPB, and poly-CMB and the effect of hydrophobicity at a 10% polymer concentration. The errors bars indicate the SD of the mean. ***P < 0.001, NS: not statistically different

Figure 7. Effects of poly-(MAA-DMAEMA), poly-SPB, and poly-CMB on the gel-to-liquid-crystalline-transition temperature of EPC at polymer/EPC mass ratios between 0 and 1.0

Figure 8. (a) ESR spectra of 5-DSA (1 mol%) incorporated into EPC in the presence of various polymers at different polymer concentrations. The numbers shown denote the order parameter (S). (b) The polyampholyte concentration dependence of the order parameter S for 5-DSA (1 mol %) intercalated into unilamellar dispersions of EPC in PBS buffer (pH 7.4).

Figure 9. (a) ESR spectra of 16-DSA (1 mol %) intercalated into EPC in the presence of various polymers at different polymer concentrations. The numbers shown denote the correlation time (τ). (b) The polyampholyte concentration dependence of correlation time τ for 16-DSA (1 mol %) intercalated into unilamellar dispersions of EPC in PBS buffer (pH 7.4)

Figure 10. Concentration dependence of hydrophobic polyampholytes (with 5% OcMA) on the correlation time τ for 16-DSA (1 mol %) intercalated into unilamellar dispersions of EPC in PBS buffer (pH 7.4)

Figure 11. Schematic representation of membrane-polyampholyte interaction/localization

Figure 12. Protection of liposomes during freezing by different polyampholytes. CF leakage from liposomes cryopreserved with various polyampholytes solutions at different polymer concentrations. Data are expressed as the mean ± SD for 3 independent experiments (5 samples each).

Figure S1. Time-dependent ^{1}H-NMR spectra of (a) poly-(MAA-DMAEMA), (b) poly-SPB and (c) poly-CMB in D_2O

Figure S2. NMR signal assignment of (a) poly-(MAA-DMAEMA), (b) poly-SPB, or (c) poly-CMB in D_2O

Figure S3. DSC heating thermograms of EPC liposomes in the presence of different amounts of (a) poly-(MAA-DMAEMA), (b) poly-SPB, or (c) poly-CMB. The resulting polymer/EPC mass ratios are indicated to the right of each trace.

Table S1. Polymer contact angle and viscosity of various polymers, with and without their hydrophobic derivatives at a 2.5% polymer concentration

TOC figure

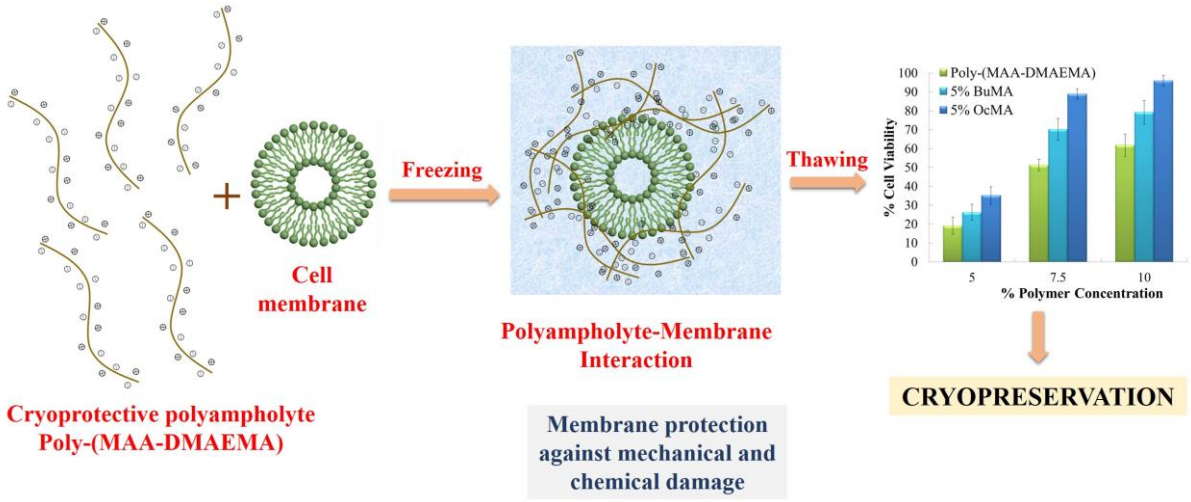
Cell membrane
Freezing
Thawing
Poly-(MAA-DMAEMA)
5% BuMA
5% OcMA
% Cell Viability
% Polymer Concentration
Cryoprotective polyampholyte Poly-(MAA-DMAEMA)
Polyampholyte-Membrane Interaction
Membrane protection against mechanical and chemical damage
CRYOPRESERVATION